LAWRENCE
LIVERMORE
NATIONAL
LABORATORY

UCRL-JRNL-236816

An Integrated Method for Accurate Determination of Melting in High-Pressure Laser Heating Experiments

L. R. Benedetti, D. Antonangeli, D. L. Farber, M. Mezouar

November 27, 2007

Applied Physics Letters

Disclaimer

An integrated method for accurate determination of melting in high-pressure laser heating experiments

Laura Robin Benedetti, Daniele Antonangeli, Daniel L. Farber

Institute for Geophysics and Planetary Physics, Lawrence Livermore National Laboratory, 7000 East Ave, Livermore, CA 94550, USA

Mohamed Mezouar

ESRF, 6 rue Jules Horowitz, BP 220, F-38043 Grenoble Cedex, France

Abstract

We present an integrated approach for melting determination by monitoring several criteria simultaneously. In particular we combine x-ray diffraction observations with the detection of discontinuities in the optical properties by spectroradiometric measurements. This approach significantly increases the confidence of melt identification, especially with low-Z samples. We demonstrate the method with observations of melt in oxygen at 47 and 55 gigapascals.

The determination of melting temperatures in the laser-heated diamond-anvil cell (LHDAC) is of broad interest for basic as well applied sciences, with direct relevance to earth science, materials science, and physics. However, how to accurately detect melting is a hotly debated topic. Widely used criteria indicating the onset of melting include: visual observation [1, 2], laser speckle analysis [3, 4], change in slope in observed temperature as a function of laser power [5], and x-ray diffraction[6,7]. Each method has serious drawbacks. The direct visual and speckle methods are subjective, and it becomes difficult to distinguish motion from flicker at high temperatures when emission is very strong. Kinks in temperature vs. power may be due to many factors, including solid-solid phase transformation. The disappearance of Bragg reflections may be caused by crystallite reorientation, solid-solid phase transformations, or melting, while the observation of the diffraction pattern of a fluid -- unambiguous proof of melt -- is weak compared to the diffraction peaks of a crystalline solid, and often difficult to distinguish from the background signal.

In this letter we augment the x-ray diffraction methods of determining melting by introducing an approach that takes advantage of the ability in modern high-pressure x-ray diffraction facilities to simultaneously monitor several physical parameters. Unambiguous direct detection of melting by x-ray diffraction is, at best, at the limit of modern experimental capabilities, especially in the case of low-Z samples that weakly diffract x-rays. Nevertheless, it is indispensable: among the methods listed above, only x-ray diffraction provides direct information about the physical state of the sample. In addition to monitoring diffraction, here we incorporate spectroradiometric data normally

used for temperature measurement to monitor the sample's optical properties. We demonstrate that monitoring both structural and optical properties simultaneously is superior to any single method for determining melting temperature. As an example of this, we present optical measurements of oxygen (Z=8) laser heated at 47 and 55 GPa.

The method we propose here uses spectroradiometric data to infer optical properties that are related to sample emissivity. We took care to minimize axial temperature gradients as these could potentially bias thermal-emission spectra. Samples of pure oxygen were pressurized to ~50 GPa in a diamond anvil cell using a new double-sample-chamber geometry that acted to significantly limit thermal gradients in the axial direction (Figure 1). Simultaneous double-sided laser heating and x-ray diffraction experiments were conducted at the ESRF beamline ID27 [8,9]. The oxygen samples were heated by direct absorption of the Nd:YAG (λ = 1064 nm) laser. Temperatures were determined and spectroradiometric uncertainties estimated following the methods outlined in [10]. The center of the laser-heated hotspot and the focus of the spectroradiometric apparatus were aligned using the x-ray fluorescence from the Re gasket. During heating, the laser and spectrometer were constantly monitored to maintain a position in line with the x-rays. The x-ray position relative to the optics was further checked before and after each heating cycle.

Evidence of melting determined from X-ray diffraction includes two distinct observations: 1) the observation of the broad diffraction signature of a fluid (affirmative) and 2) the loss of Bragg diffraction (negative). The loss of Bragg peaks associated with destruction of long range crystallographic order by melting should be a necessary, but not sufficient, condition for an x-ray-diffraction-based determination of melting, while

simultaneous observation of the broad fluid signature is unambiguous proof of the presence of melt. However, in practice, capturing both components simultaneously is extremely difficult. Fluid diffraction is an order of magnitude weaker in intensity than solid diffraction, requiring long exposures and high dynamic range detectors (which typically also have slow readout). In contrast, we find that complete loss of Bragg reflections associated with melting is a transient phenomenon, requiring many extremely rapid observations to capture it. This is due to the dynamic character of liquids: when the sample melts, the Bragg peaks from the solid sample disappear, and soon afterward, the presence of radial temperature gradients in concert with the lower liquid viscosity promotes convection, wherein small crystallites of colder material are transported into the path of the x-ray beam and heating laser. New Bragg peaks appear in the diffraction pattern then, until these crystallites reach the hotspot-temperature and melt. This dynamic process -- which is characteristic of the fluid phase and is not due to technical problems with sample alignment or dimensions of the hotspot -- interferes with the clear time independent observation of unique melting conditions. Fortunately, if several observations are made rapidly with a two-dimensional detector, the motion of small crystallites can be observed and is distinguishable from the static diffraction of a bulk solid. Diffraction from these small, entrained crystallites tends to be narrower and composed of many small spots, distinctly different from the diffraction patterns of bulk high-pressure powders. In addition, the position of the spots moves along the Debye ring, as small crystallites translate across or rotate in the x-ray beam.

The high brilliance of third generation x-ray sources such as the ESRF allows the acquisition of a high-quality diffraction pattern with only 1-2 seconds collection for high

Z elements (*e.g.* Pb, Fe). Thus, for these materials, a rapid sequence of exposures (using a fast readout ccd camera) can capture the transient loss of Bragg diffraction and subsequent motion of cold crystallites while also providing adequate signal-to-noise to observe the weaker diffraction of the fluid [11]. While this method is promising, it may only prove useful for the limited class of materials that are extremely strong diffractors.

Our experiments on oxygen (Z=8) required at least 50 s of acquisition time to record adequate patterns of the solid phase. Thus, the timescales necessary to observe signal from the fluid were longer than the characteristic timescale of crystallite motion in the sample chamber and at times longer than the timescale over which temperature stability in the samples could be maintained. Consequently, while we collected over 80 high-temperature diffraction patterns at four different pressures the unambiguous determination of melt by the simple observation of the fluid diffraction was consistently inhibited. However, by collecting data as rapidly as possible, we could observe the *transient* loss of Bragg diffraction during laser-heating. For example, at 55 GPa and 1400 K an abrupt increase of laser power (by adding the second laser) caused a large temperature excursion to 2300 K, at which temperature two 50-second diffraction patterns show little to no diffraction of ε-oxygen. However, the subsequent diffraction pattern (with no change in laser power or temperature) contained the four reflections characteristic of the solid phase before melting. In these patterns, the reflections were distinctly narrower and spotty, indicating diffraction from entrained crystallites. As laser power was increased, the next few diffraction patterns show the spots from those reflections rotating along the constant two-theta ring, again indicating physical motion of the diffracting crystallites.

In order to enhance our interpretations, we introduce an optical properties based criteria of the fusion curve determination, by analysis of the thermal emission spectra. Thermal emission intensity satisfies the Planck distribution and can be linearized to the Wien approximation with accuracy loss of less than a few percent [10]

$$I_{Wien} = \frac{k}{hc}\ln\left(I_{Planck}\frac{\lambda^5}{2\pi hc^2}\right) \approx \frac{k}{hc}\ln\varepsilon(\lambda) - \frac{1}{\lambda}\frac{1}{T} \qquad (1)$$

where I_{planck} is the thermal emission intensity, h is Planck's constant, c is the speed of light, k is Boltzman's constant, T is temperature, λ is wavelength of light, and ε is the emissivity of the material emitting thermal radiation. Assuming that ε has no wavelength dependence (gray-body approach), the temperature may then be determined by a simple linear least-squares fit where the independent variable is $1/\lambda$, the fitted slope is then $1/T$, and the fitted intercept is $k\ln\varepsilon/hc$.

Least-squares fitting to a linear function, $y=ax+b$, is independent of algorithm or initial guess: the fit parameters a and b are simple summations:

$$a_{fit} = \frac{n\Sigma xy - \Sigma x\Sigma y}{n\Sigma x^2 - (\Sigma x)^2} \text{ and} \qquad (2)$$

$$b_{fit} = \frac{n\Sigma y\Sigma x^2 - \Sigma x\Sigma xy}{n\Sigma x^2 - (\Sigma x)^2} \qquad (3)$$

The effect of non-linearity in the data, i.e., $y=ax+b(x)$, is similarly calculable by substitution into Eqs 2 and 3:

$$a_{fit} = a + \frac{\Sigma xb(x) - \Sigma x\Sigma b(x)}{n\Sigma x^2 - (\Sigma x)^2} \qquad \text{and} \qquad (4)$$

$$b_{fit} = \frac{\Sigma b(x)\Sigma x^2 - \Sigma x\Sigma xb(x)}{n\Sigma x^2 - (\Sigma x)^2} \quad . \qquad (5)$$

Thus, both b_{fit} and the quantity $(a-a_{fit})$ are independent of a, and only functions of $b(x)$. Consequently, the residual of a fit, R, is a function purely of $b(x)$ also:

$$R = \left(ax + b(x)\right) - \left(a_{fit}x + b_{fit}\right) = \left(a - a_{fit}\right)x + \left(b(x) - b_{fit}\right) \tag{6}$$

Returning to the spectroradiometric application, $a=1/T$ while $b(x)=k\ln\varepsilon(\lambda)/hc$, and the residual of Wien fitting to spectroradiometric data is,

$$R = \frac{k}{hc}\left[\ln\left(\varepsilon(\lambda)\right) - \ln(\varepsilon_{fit})\right] - \frac{1}{\lambda}\left[\frac{1}{T} - \frac{1}{T_{fit}}\right] \tag{7}$$

$$R(\lambda) = \frac{k}{hc}\left[\ln\left(\varepsilon(\lambda)\right) - \ln(\varepsilon_{fit}) + \frac{1}{\lambda}\frac{\sum\frac{\ln\varepsilon(\lambda)}{\lambda} - \sum\frac{1}{\lambda}\sum\ln\varepsilon(\lambda)}{n\sum\left(\frac{1}{\lambda}\right)^2 - \left(\sum\frac{1}{\lambda}\right)^2}\right] \tag{8}$$

a function only of $\varepsilon(\lambda)$, and not of T. Similarly, the accuracy of the temperature measurement, as expressed by the quantity $(1/T_{actual} - 1/T_{fit})$ is also independent of temperature.

In a spectroradiometric estimate of temperature, changes in absorbance, transmittance, and reflectance are indistinguishable from changes in emissivity. Thus, monitoring the residual of the Wien fit to the emission spectra provides a direct measurement of average optical properties. Although not a direct observation of melting (as a solid-solid phase transition may also be accompanied by a change in optical properties), the combined observation of changes in optical properties in concert with crystallite motion and the loss of Bragg diffraction, strongly supports interpretation of a melting transition. Moreover, in low-Z materials these changes are *easier* to observe than structural changes because the collection time of spectroradiometry is much shorter than for diffraction (about 100 spectroradiometry measurements were collected during one

laser heating cycle, as compared to 16 diffraction measurements).

In support of this approach, we note that many materials exhibit changes in optical properties upon melting [12]. Oxygen in particular, is a good candidate to test the method as it exhibits pressure-dependent variations in wavelength-dependent absorbance [13]. Figure 2 shows a typical Wien function plot and linear fit, together with the residual. In the bottom panel of figure 2, eight residual Wien functions at different temperatures during one laser heating cycle (55 GPa) are plotted. Clear changes are evident in the residual of the Wien function during the laser-heating of oxygen: Temperatures below our observed melting point (1850 K ± 450K) all have a concave down residual, while temperatures higher than our T_{melt} all have a concave-up shaped residual. These changes are plausibly related to the shift of the absorption edge from the red to the infrared

Thus, in order to determine melting, we use the concurrence of several phenomena: 1) the loss of x-ray diffraction of O_2 solid Bragg peaks; 2) the onset of sample motion evidenced by x-ray diffraction; 3) the onset of sample motion evidenced by visual inspection; and 4) the change in optical properties, determined during spectroradiometry. In our case, while we laser-heated at four different pressures, we observed all four of these criteria only at 55 GPa. At 47 GPa, we did not observe complete loss of Bragg peaks, possibly due to longer x-ray diffraction exposures. However, concurrently with both visible and x-ray diffraction evidence for the onset of motion, we did see an optical transition nearly identical to that at 55 GPa for temperatures above 1500 ± 200 K. Thus, we take this point to be the melting temperature at 47 GPa. We find that the two additional criteria we have described (evidence of motion by x-ray diffraction and

evidence of change in optical properties by spectroradiometry) significantly improves the confidence in determining a unique melting temperature, and we suggest that careful monitoring of these multiple criteria be utilized for improving the accuracy of melting temperature determinations.

Acknowledgements: Chantel Aracne and Dave Ruddle provided essential technical support. This work performed under the auspices of the U.S. Department of Energy by Lawrence Livermore National Laboratory under Contract DE-AC52-07NA27344. We acknowledge the European Synchrotron Radiation Facility for provision of synchrotron radiation facilities and we would like to thank Guillaume Morard and Jean-Philippe Perrillat for assistance in using beamline ID27.

References

[1] R. Jeanloz and A. Kavner, Phil. Trans. R. Soc. Lond. A **354**, 1279 (1996).

[2] Q. Williams, E. Knittle, and R. Jeanloz, J. Geophys. Res **96**, 2717 (1991).

[3] R. Boehler, Phil. Trans. R. Soc. Lond. A **354**, 1265 (1996).

[4] A. P. Jephcoat and S. P. Besedin, Phil. Trans. R. Soc. Lond. A **354**, 1711 (1996).

[5] P. Lazor and S. K. Saxena, Phil. Trans. R. Soc. Lond. A **354**, 1307 (1996).

[6] M. R. Frank, Y. Fei, and J. Hu, Geochim. et Cosmochi. Acta **68**, 2781 (2004).

[7]. D. Errandonea, M. Somayazulu, D. Häusermann, and H. K. Mao, J. Phys. Condens. Matter **15**, 7635 (2003).

[8] M. Mezouar, W. A. Crichton, S. Bauchau, F. Thurel, H. Witsch, F. Torrecillas, G. Blattmann, P. Marion, Y. Dabin, J. Chavanne, O. Hignette, C. Morawe, and C. Borel, J.

Synch. Rad. **12**, 659 (2005).

[9] E. Schultz, M. Mezouar, W. Crichton, S. Bauchau, G. Blattmann, D. Andrault, G. Fiquet, R. Boehler, N. Rambert, B. Sitaud, and P. Loubeyre, High Press. Res. **25**, 71 (2005).

[10] L. R. Benedetti and P. Loubeyre, High Press. Res. **24**, 423 (2004).

[11] A. Dewaele, M. Mezouar, N. Guignot, and P. Loubeyre, Phys. Rev. B, **76**, 144106 (2007).

[12]H. Watanabe, M. Susa, H. Fukuyama, and K. Nagata, High Temp. – High Press. **31**, 587 (1999).

[13] M. Nicol, and K. Syassen, Phys. Rev. B, **28**, 1201 (1983).

Figures and Captions.

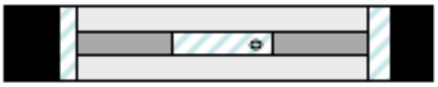

Figure 1. Cross section of the sample chamber geometry. Inside the sample chamber created by the diamond anvils and Re gasket (black), the oxygen sample (///, cross hatching) was contained by a secondary interior sample chamber composed of two single-crystal Al_2O_3 discs (light gray) and an annulus of gold (dark gray). A single ruby sphere inside the interior sample chamber was used to monitor pressure.

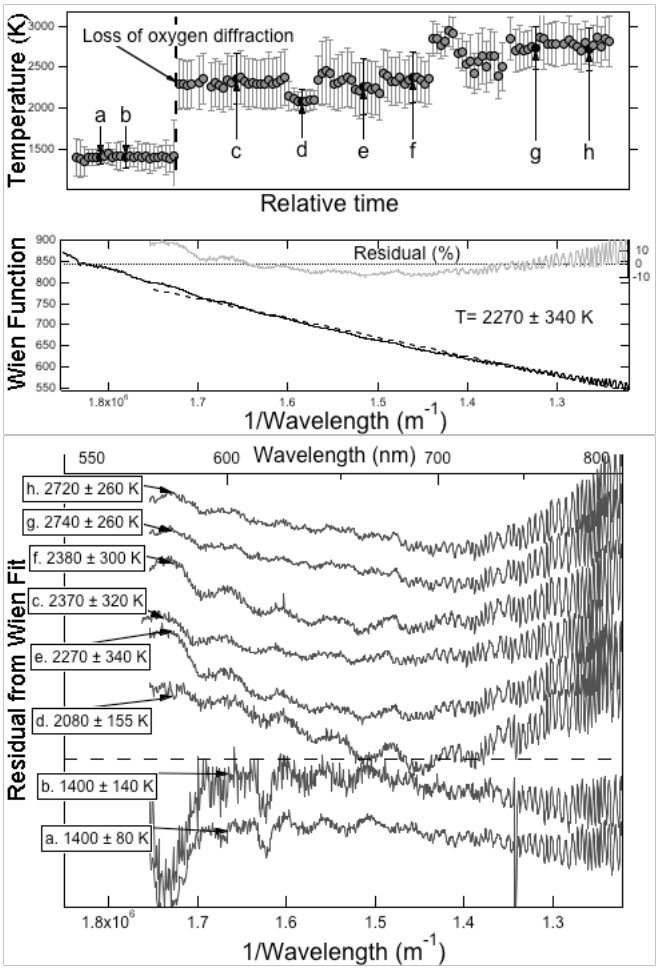

Figure 2. Spectroradiometric observations. (**top**) Melting was observed, along with a large temperature jump from 1400 K to 2080 K, when the second laser was turned on. Observations referenced in the bottom panels are marked with the letters a-h. (**middle**) Observed Wien function and fit at point ***e***. (**bottom**) Residuals to the Wien fit at eight temperatures. The wavelength dependence of the residual changes significantly above and below our observed melting point (dashed line).